Title

EVALUATION OF CURRENT DISTRIBUTION ELECTRODE SYSTEMS BY HIGH-SPICED DIGITAL COMPUTERS

Authors

Klingert, Jack A.
Scott, Lynn
Tobias, Charles W.

Publication Date

1963-09-01

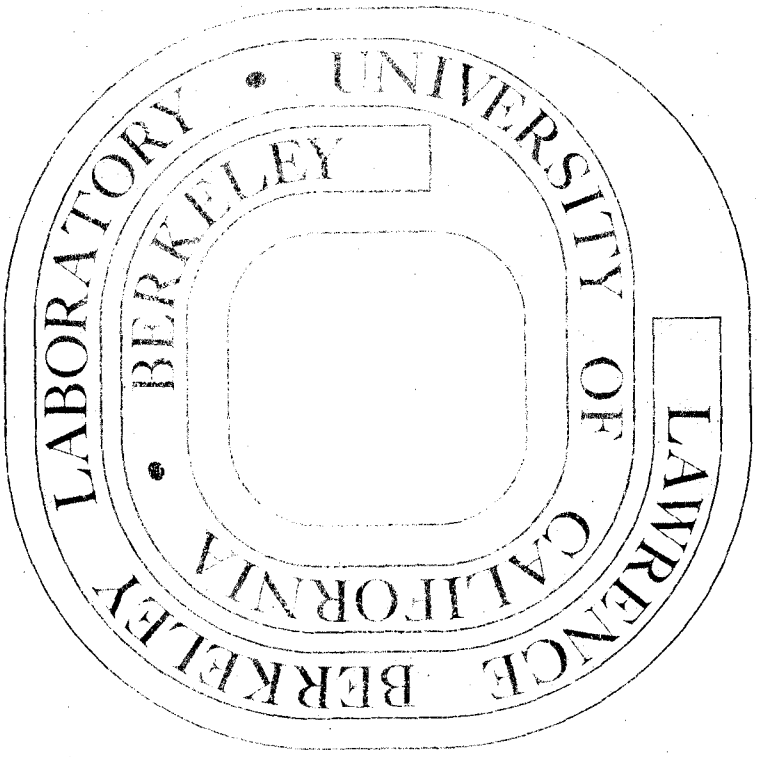

DISCLAIMER

UCRL-10998

UNIVERSITY OF CALIFORNIA

Lawrence Radiation Laboratory

Berkeley, California

AEC Contract No. W-7405-eng-48

EVALUATION OF CURRENT DISTRIBUTION IN ELECTRODE SYSTEMS BY HIGH-SPEED DIGITAL COMPUTERS

Jack A. Klingert, Scott Lynn, and Charles W. Tobias

September 1963

Evaluation of Current Distribution in Electrode Systems by High-Speed Digital Computers

Jack A. Klingert, Scott Lynn, and Charles W. Tobias

Lawrence Radiation Laboratory
and
Department of Chemical Engineering
University of California, Berkeley, California

ABSTRACT

In the absence of significant concentration gradients, the distribution of potential in electrolytic cells can be satisfactorily described by the Laplace equation. Because of severe mathematical difficulties, in the past, analytical solutions have been obtained only for a few, simple cell configurations. In other fields of application it is well known that the finite-difference form of the Laplace equation by iterative procedure is ideally suited for numerical solution by digital computers. The method is suitable for handling any arbitrary two-dimensional cell geometry, and allows consideration of realistic overpotential behavior.

Brief description is given of the elementary mathematical relations involved, and of the iterative procedure employed in machine computations. By use of this technique, the primary and secondary current density distributions were evaluated for the outside corner of an electrode, a model representative of cell geometries commonly employed in industry. The effects of the variations of geometric and overpotential parameters are demonstrated. The results obtained indicate that the numerical technique employed is eminently suitable for rapid and accurate evaluation of current density distributions for realistic models.

UCRL-10998

Evaluation of Current Distribution in Electrode Systems by High-Speed Digital Computers*

Jack A. Klingert, Scott Lynn+, and Charles W. Tobias

INTRODUCTION

The determination of current density distribution, and its dependence on cell geometry, on solution properties, on hydrodynamic conditions, and on the impedances associated with charge-transfer reactions has long been recognized to be of importance in the design and conduct of metal deposition and dissolution processes. In more recent years, the need for more rational procedures for the prediction of performance of industrial electrolytic processes and of various galvanic cell types has become increasingly evident.

The problem in its most general formulation includes the consideration of concentration gradients associated with the progress of electrode reactions.[1] However, in numerous applications, the bulk electrolyte is well stirred, and its composition may be assumed invariant. Further, the concentration gradients near the electrode surfaces may be small, and therefore their influence on the electrode potential can be considered negligible. Under these conditions, the local electrode potential is dependent only on the activation overpotential corresponding to the local current density.[2] The distribution of potential between the electrodes then can be described by the Laplace equation,

$$\nabla^2 E = 0.$$

In 1940, Kasper[2,3,4,5] presented an orderly and lucid exposition of the boundary conditions pertaining to metal deposition and dissolution processes, neglecting mass transport effects. Methods of obtaining

solutions for various types of electrode geometries were described by (among others) Wagner,[6,7] Kronsbein,[8] and Drossbach.[9,10] Agar and Hoar,[11] Wagner,[6,7] and Wijsman and Tobias.[12] discussed the significant parameters, and the criteria of similarity.

Analytical solutions of the Laplace equation have been obtained for a number of simple cell geometries.[3,4,5,6,8] Most of these solutions evaluate only the primary distribution,[2] i.e. disregard any overpotential effects at the electrodes. Consideration of linear or logarithmic overpotential relationships leads to more severe mathematical difficulties.[6,7,12,13] Instead of solving the Laplace equation, it is possible then to employ integral equations to evaluate the local current densities.[13,14] More complicated electrode geometries required model experiments with the electric trough, or application of graphical techniques of potential mapping.[15] Unfortunately both these techniques are quite inaccurate when sharp variations of potential occur over very small distances. Further, neither of these techniques allows the consideration of overpotential effects.

Although much progress has been made during the last 20 years in understanding current distribution phenomena, and in obtaining solutions to certain simple problems, there appears to be a definite need for more convenient methods to solve problems of higher degrees of complexity. Further, it is desirable to introduce techniques that do not require unusual mathematical skills, excessive time, or elaborate (although not very accurate) experimental methods. These criteria appear to be met by the method of the iterative solution of the difference form of the Laplace equation.

APPLICATION OF THE DIFFERENCE FORM OF THE LAPLACE EQUATION TO SOLVING PROBLEMS IN CURRENT DISTRIBUTION

Various techniques for the evaluation of temperature, stress, and flow fields by numerical methods have been perfected in the past several decades. The most commonly employed method involves the numerical solution of the difference form of the laplace equation by "iteration" or "relaxation."[16,17,18] In the following the basic features of this method are outlined, and the typical boundary conditions representative of electrolytic cell systems are introduced.

Basic Considerations

By replacing the differential equation

$$\nabla^2 E = \frac{\partial^2 E}{\partial x^2} + \frac{\partial^2 E}{\partial y^2} = 0 \qquad (1)$$

with the difference equation

$$\frac{\Delta_c E^2}{(\Delta x)^2} + \frac{\Delta_c E^2}{(\Delta y)^2} = 0, \qquad (2)$$

we replace the description of a continuum with a rectangular network (Fig. 1). The meaning of the central difference quotients in equation (2) may be understood with reference to Fig. 2. Here the values of the forward and backward difference quotients are

$$\frac{\Delta_f E}{\Delta x} = \frac{E_1 - E_0}{h} \quad \text{and} \quad \frac{\Delta_b E}{\Delta x} = \frac{E_0 - E_3}{h},$$

respectively. The second central difference quotient then is given by

$$\frac{\Delta_c E^2}{(\Delta x)^2} = \frac{\frac{\Delta_f E}{\Delta y} - \frac{\Delta_b E}{\Delta x}}{h} = \frac{E_1 - 2E_0 + E_3}{h^2}. \qquad (3)$$

By similar reasoning,

$$\frac{\Delta_c E^2}{(\Delta y)^2} = \frac{\frac{\Delta_f E}{\Delta y} - \frac{\Delta_b E}{\Delta y}}{h} = \frac{E_2 - 2E_0 + E_4}{h^2}. \qquad (4)$$

Addition of equations (3) and (4) results in the remarkably simple relationship

$$E_o = \frac{E_1 + E_2 + E_3 + E_4}{4} \quad . \qquad (5)$$

Thus we obtain a simple formula that relates the potential at each point of the grid to the potentials at the four nearest neighbors. If we satisfy the condition stated in equation (5) simultaneously at every grid point within the regime considered, we obtain a solution to equation (2), the difference form of the Laplace equation.*

We will briefly consider now the degree of approximation involved in substituting the difference equation (equation 2) for the differential equation (equation 1). With reference to Fig. 2, Taylor expansion of the potential function with respect to both x and y about point 0, with interval h, results in

$$\frac{\Delta_c E^2}{(\Delta x)^2} + \frac{\Delta_c E^2}{(\Delta y)^2} = \nabla^2 E + \frac{2h^2}{4!}\nabla^4 E + \frac{2h^6}{6!}\nabla^6 E + \ldots \quad . \qquad (6)$$

Thus the error committed in setting the left-hand side equal to zero is represented by a power series that converges rapidly, and for a small mesh interval, h, the first term of the series involving h^2 is already negligible.[17]

Boundary conditions

In addition to the formula relating the potential at each point of the grid to those at its neighbors, we also have to state the conditions at the boundaries in difference form.

---

* It should be noted that instead of the simplest "square" or "cross" formulae, represented by equation (5), larger "molecules" involving the nearest eight or nineteen neighbors can be developed. Solutions employing these higher-order approximations approach the solution of the differential equation even more closely than those involving equation (5).[18]

a. For conducting boundaries, in the absence of an overpotential dependent on current density, we specify the potential of the electrode, E_c which is usually uniform. Thus in Fig. 3, if the four sides of the quadrangle were electrodes at different potentials, we would write down at each boundary point along the four different sides the corresponding values of the potential.

b. For insulating boundaries, the normal flux is zero. In this case we construct image points behind the boundary (points 1', 2', 3', 4', in Fig. 4), and set the potentials at these points equal to their counterparts within the regime considered. Thus

$$E_1' = E_1,\ E_2' = E_2,\ \text{etc.}$$

The mesh points on the boundary will then be treated as any interior point. For instance, at point B_3 in Fig. 4, the potential is calculated by

$$E_{B_3} = \frac{2E_3 + E_{B_2} + E_{B_4}}{4}$$

c. The third type of boundary condition describing electrodes with current-dependent overpotential concerns the case in which neither the potential nor the current is specified at the boundary, only their functional relationship. The finite-difference expression will, of course, depend on the relation specified between current and potential (Fig. 5).

For linear overpotential relations, the potential in the electrode, E_c, is related to the potential on the solution side, E_B, by

$$E_B = E_c - b \cdot i.$$

Therefore,

$$E_B = E_c - \frac{b \cdot K}{h}(E_B - E_1), \text{ and } E_B = \frac{E_c - \frac{b \cdot K}{h} E_1}{1 + \frac{b \cdot K}{h}}, \qquad (7)$$

where b = slope of i vs E line, $\Omega\,cm^2$, K = conductivity of electrolyte $\Omega^{-1}cm^{-1}$.

For a logarithmic relationship between potential and current density (Tafel polarization), the relation of the local density of the current to the exchange-current density must be taken into consideration:

$$E_B = E_c - \beta \cdot \ell n \frac{i}{i_o} = E_c - \beta \cdot \ell n \frac{(E_B - E_1) K}{i_o \cdot h}, \qquad (8)$$

where $\beta = \frac{RT}{\alpha nF}$ volts, i_o = exchange current and density A/cm^2, and α = transfer coefficient. Evaluation of the potential at the solution side of the boundary in this case involves a trial-and-error procedure.

Method of solution

As shown in the preceding section, it is possible to write an equation for every point of the rectangular grid, including the points on the boundaries. These equations must be solved simultaneously to specified limits of accuracy.

The simplest procedure, the method of iteration, involves a progressive self-correcting solution, starting with the values given at the boundaries and arbitrarily assumed values of the potential in the interior of the grid. Consider the rectangular regime in Fig. 3. Let us assume that in this problem all values of the potential are specified at the boundaries. We shall write in reasonable values of the potential at each grid point and then, using equation (5), calculate a new value, E'_8, for point 8, and using this new value, calculate E'_9 for point 9, etc. Using the improved values generated, we proceed in an orderly manner as indicated in Fig. 3, and, after a full sweep through the regime

considered, we return to point 8, etc. This procedure is continued until at each mesh point the basic relationship, equation (5), is approached to within the specified error limit ϵ:

$$\epsilon > \left| E_o - \frac{E_1 + E_2 + E_3 + E_4}{} \right| \geq 0$$

The maximum possible error that we can introduce by allowing an error smaller than ϵ at each point within a regime bound by a circle of radius r cannot exceed $\frac{\epsilon}{4}(\frac{r}{h})^{2.16}$ For example, if r/h = 50, and $\epsilon = 10^{-6}$ volt, the maximum possible error at a grid point will be less than 4×10^{-4} volt. An appropriate check may be made of the accuracy of the solution if one refines the grid and compares the values calculated for the finer grid with those obtained earlier.

The calculation procedure for cases involving insulating boundaries, and electrodes with overpotential condition, becomes necessarily more involved. However, powerful numerical techniques are available for the solution of equation (8)[20] and the computation will again involve only routine manipulations.

To obtain sufficiently accurate solutions, a fine grid and low error limits for the solution of equation (5) must be used. In general, the grid intervals should be small compared with the distances over which a significant variation of flux occurs. In practice, we find that grids containing from a few hundred to a few thousand points are required. The number of sweeps, or passes, will vary according to the geometry of the problem and the overpotential relations employed. In a typical case, from several hundred to several thousand passes are required to solve a problem of average complexity. Thus somewhere between 10^4 and 10^7 individual grid-point solutions are required to obtain a single distribution. Although

these numbers appear formidable, since the calculations outlined above are ideally suited for programming onto high-speed digital computers, highly accurate solutions may be obtained quite rapidly. Depending on the accuracy desired and the complexity of the problem, the average time involved on an IBM 7090 computer is in the range of a few minutes to a fraction of an hour.

CURRENT DISTRIBUTION IN AN L-SHAPED REGION

The geometry chosen to illustrate the numerical evaluation of current distribution is shown in Fig. 6. As is demonstrated in Fig. 7, application of sectioning rules to this basic element[2] allows the generation of many important practical cell geometries. For $a < c \ll d$, and $a \ll b$, we obtain the model of a fissure-type pore, of interest in the description of porous electrodes.

In the present exploration of this model, we have restricted the range of geometric parameters as follows:

$$c = 2d \text{ in all cases,}$$

$$b = 4d \text{ in all cases,}$$

$$d/4 < a < 2d;$$

h was chosen to be equal to d/20. The number of mesh points involved varied from 1,300 (for a=d/4) to 4,800 (for a=2d). The potential applied across the electrodes was 1.0 volt when the primary current distribution was evaluated.

In order to keep the curent density, i_r, at the right-hand corner of the anode, the same as in the primary distribution examples, an appropriately higher anode potential was used when the effect of anodic overpotential was evaluated. An error limit of 10^{-6} volt was applied in the primary distribution cases, and 10^{-4} volt for the cases involving

overpotential. The number of passes required was between 800 and 3,000.

The distribution near the corner was evaluated both with a sharp-point corner, and a rounded-off corner having a radius of d/20. For this latter case the grid near the corner was refined to h = d/80 (see shaded region in Fig. 6).

The effect of overpotential at the anode was studied by using a single length relation: a = d. In contrast to the case of primary distribution, here the relation of absolute size to conductivity and to the impedance corresponding to polarization must be considered.

As shown by Agar and Hoar[11] and Wagner,[6] in the case of linear overpotential relation the significant parameter is $\mu_L = K\, b/L$, where L is the significant dimension of the regime considered.* In evaluating the effect of linear polarization on current distribution in a given geometry, therefore, it is unnecessary to vary all three variables individually; rather it suffices to obtain solutions for a range of values of μ_L. This dimensionless number represents the ratio of the potential drop at the interface, corresponding to the current-dependent portion of the electrode potential, to the potential drop across the significant length of the system. When μ_L is small compared with unity, the current distribution approaches the primary distribution; for $\mu_L \gg 1$, the impedance corresponding to the discharge reaction dominates, and the distribution approaches uniformity.

Similar reasoning[7] leads for the case of logarithmic (Tafel) overpotential relationship to the similarity criterion

---

* For the range of geometric parameters considered here, the choice of L = d is appropriate.

$$\mu_T = \frac{K\,\beta}{L\,i},$$

where β is the Tafel slope (volts), and i is the average current density corresponding to the location of L. As shown, in this case the current distribution depends on the average current density also. Again, however, identical distribution will be obtained in two geometrically similar systems, if the values of μ_T is the same for both cases.

In our case the distribution at the anode was evaluated with μ_L = 0.05, 0.1, 0.5, and 1.0, representative of a practical range of the combination of variables frequently employed in practice. For computational purposes one is free to choose convenient values of the variables involved in μ_L and μ_T. Individual variables were chosen as shown in Table 1.

Table 1

	μ_L	E_C (volts)	E_A (volts)	K (Ω^{-1} cm^{-1})	L(=d) cm	b ($\Omega\,cm^2$)
I	0	0	1	1	1	0
II	0.05	0	1.05	1	1	0.05
III	0.1	0	1.1	1	1	0.1
IV	0.5	0	1.5	1	1	0.5
V	1.0	0	2.0	1	1	1.0

For purposes of comparison, the effect of Tafel polarization was also computed, by using conditions identical to those of case V. $i_o = 10^{-5}$ A/cm^2 was chosen, resulting in a current density of 1.0 A/cm^2 in the right-hand corner, and β was set equal to 1.0 volt.

RESULTS AND DISCUSSION

In our model the value of b was chosen deliberately so that the effect of the corner vanished near the insulating boundary (at right, in Fig. 6), and the potential gradient at this position was constant between the two electrodes. Thus the current density near this boundary corresponds to the current density one would obtain between two infinite parallel electrodes separated by the distance d. The current density, i_r, at this boundary was chosen as a reference value, and all other densities are expressed relative to it.

Figure 8 shows the primary current distribution for a = d in the region near the corner of the anode. The dashed portion of the curve indicates approximately the way in which the current density would tend toward infinity if the corner were geometrically square. The solid line was calculated with a mesh size of d/80 in the small region shown in Fig. 6 and with a radius of d/20 for the corner. The method of projecting and subsequently unfolding the anode surface to form the abscissa is illustrated in the inset in Fig. 8. This method is also used in Figs. 9 through 13.

In Fig. 9 the current distribution for the entire anode is shown on a smaller scale. An abbreviated listing of i/i_r values is given in Table 1. The current flowing into the normal branch of the anode is shown here to depend strongly on a/d. The current distribution along the cathode is remarkably uniform. Integration of the current densities along each electrode yielded values within 1% of each other.

As is shown in Fig. 8, the actual maximum in the current density at the corner does not occur at point 0 but is somewhat displaced toward the lower side of the anode. It was also found, by using the smaller mesh

to improve the precision of the calculation, that the current distribution around the corner itself is smooth and well-behaved. Using the smaller mesh size did not produce an appreciable shift in the distribution of the current relative to that obtained previously, which indicates that the precision obtained with the larger mesh was satisfactory. On the basis of these considerations the curves for the cases showing the effect of geometry (discussed above) and polarization (discussed below) were simply drawn in smoothly in the region bounded by one mesh unit on either side of zero in Figs. 9, 10 and 11. The curves so obtained are for an electrode with a corner having a radius of one mesh unit (d/20). The case of an electrode with a geometrically sharp corner is actually of no practical importance.

The effect of linear polarization on the distribution at the anode is shown in Fig. 10 and in Table 1. The effect of increasing influence of anodic overpotential is apparent; as μ_L is increased from zero to 1.0, the current flowing into the vertical branch of the anode is much increased. The sharpness of the peak of current density (which approaches infinity for $\mu_L = 0$) at the corner is reduced, and for μ=1.0, there is no longer a maximum current density at this point. Figures 11 and 12 show the position of streamlines for $\mu_L = 0$ and $\mu_L = 1$. It should be noted that the same amount of current flows between any two adjacent streamlines.

A comparison between linear and logarithmic overpotential relationship is made in Fig. 13 at $\mu_L=\mu_T=1.0$. It is apparent that the linear expression yields a much less evening effect on the distribution than does the logarithmic one. It should be noted, however, that the two cases were calculated with such a choice of b that the current densities at the

right-hand corner were equal in the two cases. If we had chosen to match the current densities in the upper corner along the vertical branch of the anode, the linear expression would have given a more even distribution than the logarithmic one. It is evident that the linear polarization expression is inadequate to represent overvoltage behavior when a substantial range of current densities occurs within a given distribution problem.

In the foregoing sections we have attempted to show the principles underlying the iterative solution of the finite-difference form of the Laplace equation, and illustrated the method by computing the distribution in a realistic geometric model, using both linear and Tafel overpotential relationships.

We have not attempted to cover in the frame of this paper various computational techniques by which the time required for the accurate evaluation of a given problem can be further reduced. It is advisable to solve a problem initially with a large mesh interval, h_1, and then, using the potential values obtained in this manner, refine the mesh to $h_2=h_1/2$. If necessary the new potential values can again be used to initiate still another solution, using now $h_3=h_2/2$ intervals. The total number of passes required when this successive mesh refinement is employed is far smaller than if the problem is solved with the finest mesh right away. One should also consider the application of different mesh densities over different segments of the domain considered, according to the more or less irregular variation of potential in these segments. It is not necessary, for instance, to use a fine mesh when the potential varies in a linear manner in a segment. The reader is referred to specialized texts on field computations for still other powerful methods by which convergence can be accelerated.[19]

right-hand corner were equal in the two cases. If we had chosen to match the current densities in the upper corner along the vertical branch of the anode, the linear expression would have given a more even distribution than the logarithmic one. It is evident that the linear polarization expression is inadequate to represent overvoltage behavior when a substantial range of current densities occurs within a given distribution problem.

In the foregoing sections we have attempted to show the principles underlying the iterative solution of the finite-difference form of the Laplace equation, and illustrated the method by computing the distribution in a realistic geometric model, using both linear and Tafel overpotential relationships.

We have not attempted to cover in the frame of this paper various computational techniques by which the time required for the accurate evaluation of a given problem can be further reduced. It is advisable to solve a problem initially with a large mesh interval, h_1, and then, using the potential values obtained in this manner, refine the mesh to $h_2=h_1/2$. If necessary the new potential values can again be used to initiate still another solution, using now $h_3=h_2/2$ intervals. The total number of passes required when this successive mesh refinement is employed is far smaller than if the problem is solved with the finest mesh right away. One should also consider the application of different mesh densities over different segments of the domain considered, according to the more or less irregular variation of potential in these segments. It is not necessary, for instance, to use a fine mesh when the potential varies in a linear manner in a segment. The reader is referred to specialized texts on field computations for still other powerful methods by which convergence can be accelerated.[19]

right-hand corner were equal in the two cases. If we had chosen to match the current densities in the upper corner along the vertical branch of the anode, the linear expression would have given a more even distribution than the logarithmic one. It is evident that the linear polarization expression is inadequate to represent overvoltage behavior when a substantial range of current densities occurs within a given distribution problem.

In the foregoing sections we have attempted to show the principles underlying the iterative solution of the finite-difference form of the Laplace equation, and illustrated the method by computing the distribution in a realistic geometric model, using both linear and Tafel overpotential relationships.

We have not attempted to cover in the frame of this paper various computational techniques by which the time required for the accurate evaluation of a given problem can be further reduced. It is advisable to solve a problem initially with a large mesh interval, h_1, and then, using the potential values obtained in this manner, refine the mesh to $h_2=h_1/2$. If necessary the new potential values can again be used to initiate still another solution, using now $h_3=h_2/2$ intervals. The total number of passes required when this successive mesh refinement is employed is far smaller than if the problem is solved with the finest mesh right away. One should also consider the application of different mesh densities over different segments of the domain considered, according to the more or less irregular variation of potential in these segments. It is not necessary, for instance, to use a fine mesh when the potential varies in a linear manner in a segment. The reader is referred to specialized texts on field computations for still other powerful methods by which convergence can be accelerated.[19]

Numerical solutions in general require a large number of individual solutions, varying each parameter, while the others are kept constant, to yield the equivalent information that is contained in an analytical solution. Generation of such a set of solutions, however, does not in most cases require excessive computer time, particularly if programs are written judiciously. At the same time one should consider that only in a few trivial cases can one obtain analytical solutions in closed forms. In most cases, an analytical solutions is either impossible or involves a number of approximations, and, in any case, yields results that still require numerical evaluation (such as complicated integrals, or slowly converging infinite series).

The numerical solution scheme presented here allows the use of any arbitrary overpotential relationship. The effect of mass-transfer polarization on current distribution can also be included. Finally, electrode resistance effects (terminal effect) can also be taken into account.

There can be no doubt about the advantages of this technique for obtaining current density distributions in any arbitrary two-dimensional cell geometry. Use of this method does not require highly specialized preparation in applied mathematics.

TABLE 2

Ratios of local local current densities on the anode, i, to the uniform current density near the right-hand corner, i_r*.

Dist. from corner (x d)	μ_L=0	0	0	0	0.05	0.1	1.0	μ_T=1.0
	$\frac{a}{b}=\frac{1}{4}$	$\frac{1}{2}$	1	2	1	1	1	1
-4.0	0.000	0.000	0.010	0.038	0.026	0.038	0.050	0.162
-3.0	0.000	0.000	0.014	0.054	0.030	0.044	0.068	0.174
-2.0	0.000	0.002	0.038	0.108	0.054	0.070	0.140	0.222
-1.0	0.002	0.032	0.144	0.260	0.158	0.174	0.328	0.344
-0.9	0.002	0.044	0.170	0.288	0.180	0.198	0.358	0.364
-0.8	0.006	0.060	0.198	0.320	0.208	0.226	0.392	0.388
-0.7	0.010	0.082	0.234	0.358	0.242	0.260	0.430	0.416
-0.6	0.018	0.112	0.278	0.404	0.284	0.296	0.470	0.446
-0.5	0.034	0.154	0.344	0.460	0.336	0.350	0.516	0.480
-0.4	0.064	0.214	0.406	0.534	0.406	0.412	0.568	0.520
-0.3	0.120	0.306	0.508	0.636	0.500	0.500	0.628	0.570
-0.2	0.232	0.452	0.668	0.796	0.640	0.624	0.702	0.630
-0.1	0.484	0.746	0.986	1.124	0.892	0.834	0.790	0.708
-0.05	0.760	1.060	1.330	1.486	1.132	1.016	0.846	0.760
+0.05	1.352	1.524	1.686	1.776	1.484	1.350	0.986	0.922
+0.1	1.126	1.312	1.420	1.482	1.328	1.254	0.990	0.936
+0.2	1.088	1.150	1.210	1.244	1.182	1.152	0.996	0.954
+0.3	1.048	1.086	1.126	1.148	1.116	1.102	0.998	0.960
+0.4	1.028	1.056	1.082	1.096	1.078	1.068	0.998	0.972
+0.5	1.020	1.036	1.054	1.066	1.054	1.048	1.000	0.978
+0.6	1.014	1.026	1.038	1.046	1.038	1.034	1.000	0.984
+0.7	1.010	1.018	1.026	1.032	1.028	1.028	1.000	0.988
+0.8	1.006	1.012	1.020	1.022	1.018	1.018	1.000	0.990
+0.9	1.004	1.008	1.014	1.016	1.014	1.014	1.000	0.992
+1.0	1.004	1.006	1.010	1.012	1.010	1.012	1.000	0.994
+2.0	1.000	1.000	1.000	1.000	1.000	1.000	1.000	0.998

* Positive multiples of d refer to distance from the outside corner along the surface parallel to the cathode, negative ones to the distance along the surface perpendicular to it.

FOOTNOTES AND REFERENCES

* Work done under the auspices of the U. S. Atomic Energy Commission
+ Research Laboratories, Western Division, Dow Chemical Company

1. V. G. Levich, Physico-chemical Hydrodynamics, Chapter IV, (Prentice-Hall, Englewood Cliffs, N. J., 1962)
2. C. Kasper, Trans. Electrochem. Soc. 77, 353 (1940).
3. C. Kasper, ibid. 77, 365 (1940).
4. C. Kasper, ibid. 78, 131 (1940).
5. C. Kasper, ibid. 78, 147 (1940).
6. C. Wagner, J. Electrochem. Soc. 98, 116 (1951).
7. C. Wagner, Plating 48, 988 (1961).
8. J. Kronsbein, ibid. 37, 851 (1950).
9. P. Drossbach, Grundrisz der allgemeinen technischen Elektrochemie, p. 151-168, Gebr. Brntraeger, Berline 1952.
10. P. Drossbach and R. Meggle, Z. Elecktrochem, 61, 415 (1957).
11. J. N. Agar and T. P. Hoar, Discussions Faraday Soc. 1, 144 (1947).
12. C. W. Tobias and R. Wijsman, J. Electrochem. Soc. 100, 459 (1953).
13. C. Wagner, Chem. Ingr.-Tech. 32, 1 (1960).
14. C. Wagner, Advances in Electrochemistry and Electrochemical Engineering II (John Wiley and Sons, New York, 1962) Chap. 1.
15. R. H. Rousselot, Repartition du Potentiel et du Courant dans les Electrolytes (1959, Dunod, Paris).
16. J. B. Scarborough, Numerical Mathematical Analysis, 2nd Ed. (Johns Hopkins Press, Baltimore, 1950).
17. G. E. Forsythe and W. R. Wasow, Finite Difference Methods for Partial Differential Equations, (John Wiley and Sons, New York, 1960).
18. A. Thom and C. J. Apelt, Field Computations in Engineering and Physics (D. Van Nostrand Company, Inc. New York, 1961).

19. L. Lapidus, Digital Computation for Chemical Engineers, (McGraw-Hill Book Company, Inc., New York, 1962) pp. 140-158.

20. L. Lapidus, ibid., pp. 288-292.

FIGURE CAPTIONS

1. Replacement of the continuum with a rectangular network.
2. Network element.
3. Typical iteration sequence.
4. Insulating boundary.
5. Conducting boundary.
6. Geometry of the model. Element covered with lattice shows region near corner, in which the potential was evaluated using a refined mesh ($h = d/80$). For the rest of the enclosure $h = d/20$ was used.
7. Typical two dimensional multiple electrode arrangements generated from the basic model in Fig. 6 using symmetry considerations.[2] The dashed lines may be substituted by insulators, the dotted ones representing equipotential surfaces by electrodes.
8. The relative current density, i/i_r at the outside corner on the anode.
9. The effect of varying the ratio a/d on the current distribution.
10. The effect of linear polarization on current distribution.
11. Potential-flux map showing the primary distribution ($\mu=0$).
12. Potential-flux map showing the secondary distribution for $\mu_T = 1.0$.
13. Comparison of the effect of linear-, and Tafel polarization.

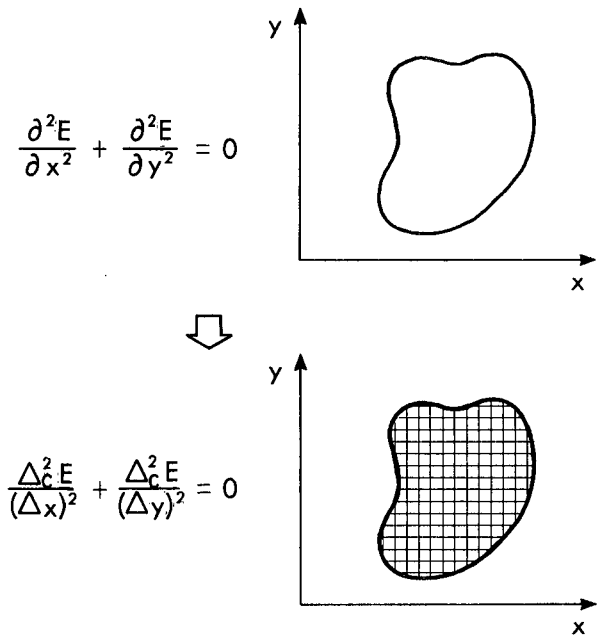

REPLACEMENT OF THE CONTINUUM WITH A RECTANGULAR NETWORK

MU-31819

Fig. 1

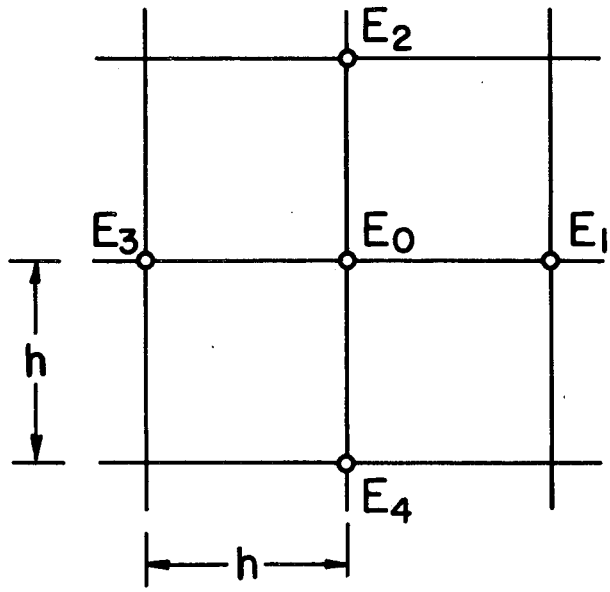

NETWORK ELEMENT

MU-31820

Fig. 2

TYPICAL ITERATION SEQUENCE

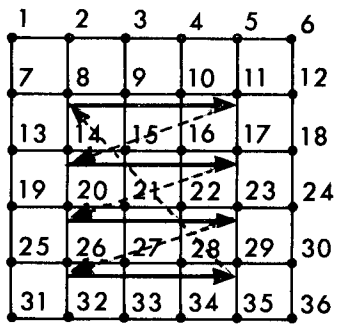

$$E'_8 = \frac{E_9 + E_2 + E_7 + E_{14}}{4}$$

$$E'_9 = \frac{E_{10} + E_3 + E'_8 + E_{15}}{4}$$

$$\vdots$$

$$E'_{14} = \frac{E_{15} + E'_8 + E_{13} + E_{20}}{4}$$

$$\vdots \quad \text{etc.}$$

MU-31818

Fig. 3

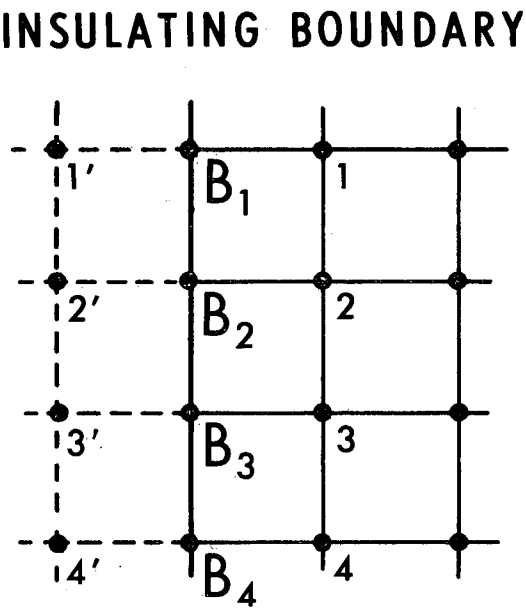

Fig. 4

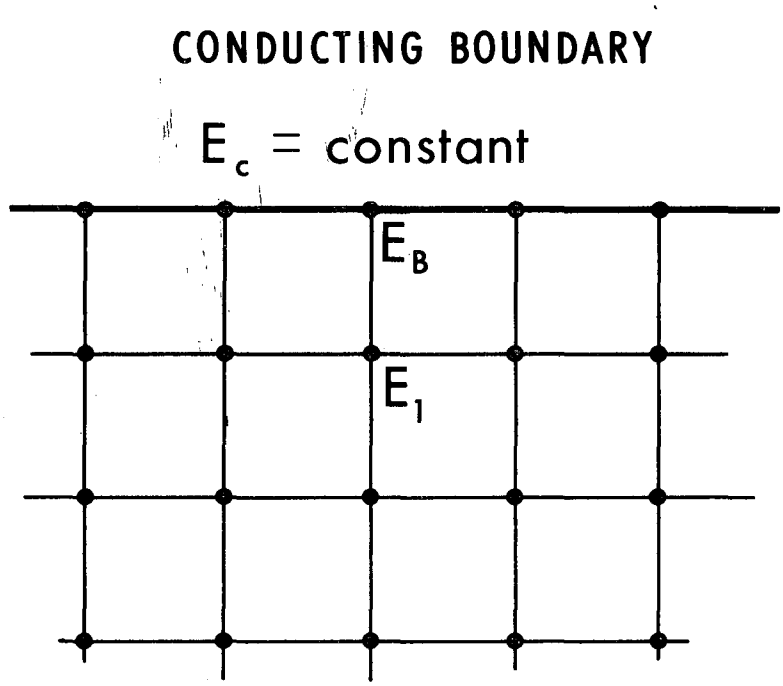

Fig. 5

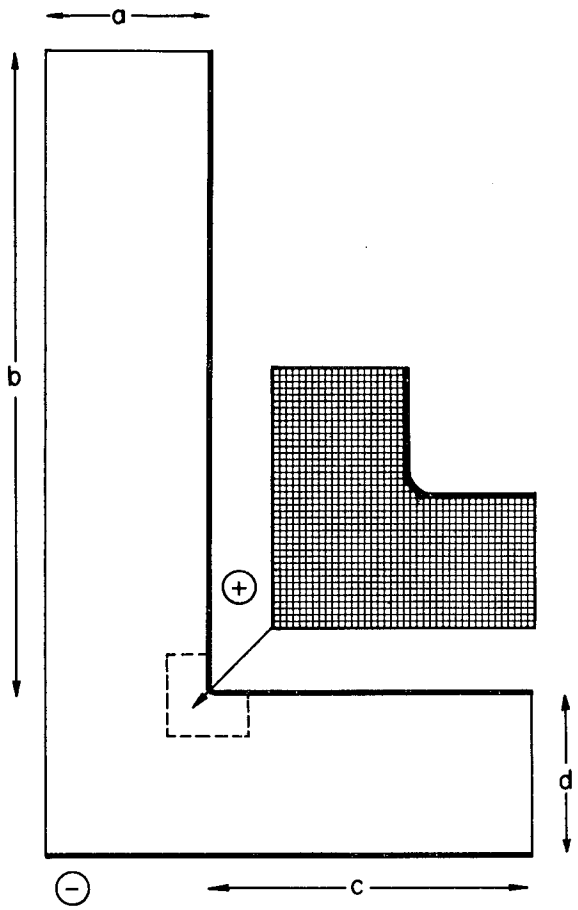

GEOMETRY OF THE MODEL

MU-31823

Fig. 6

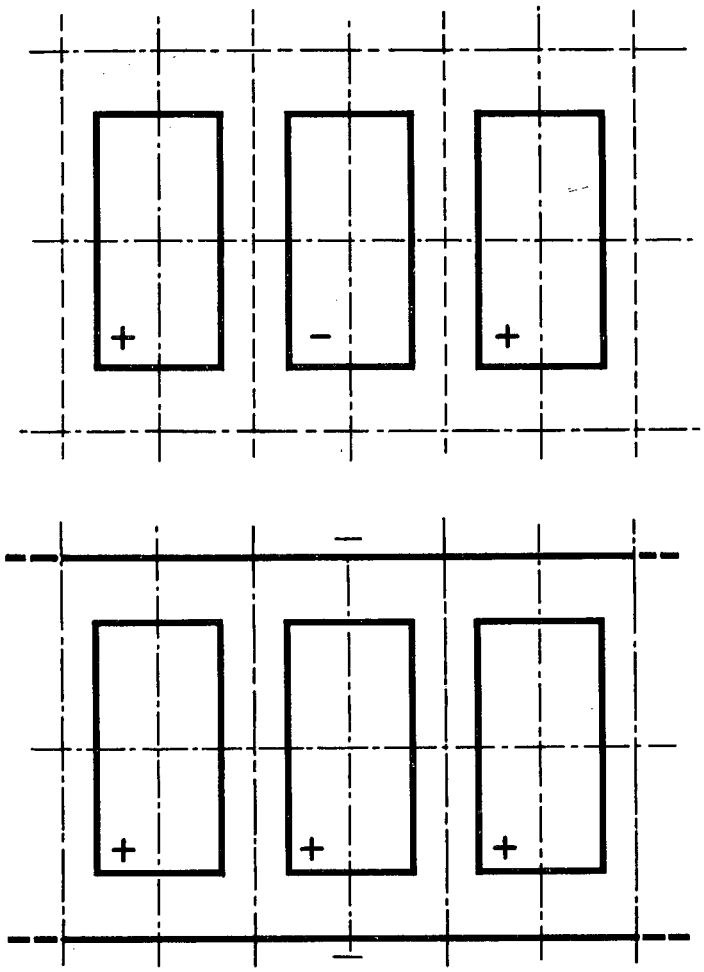

TYPICAL GEOMETRIES THAT
ONE CAN GENERATE BY BASIC MODEL

MU-31824

Fig. 7

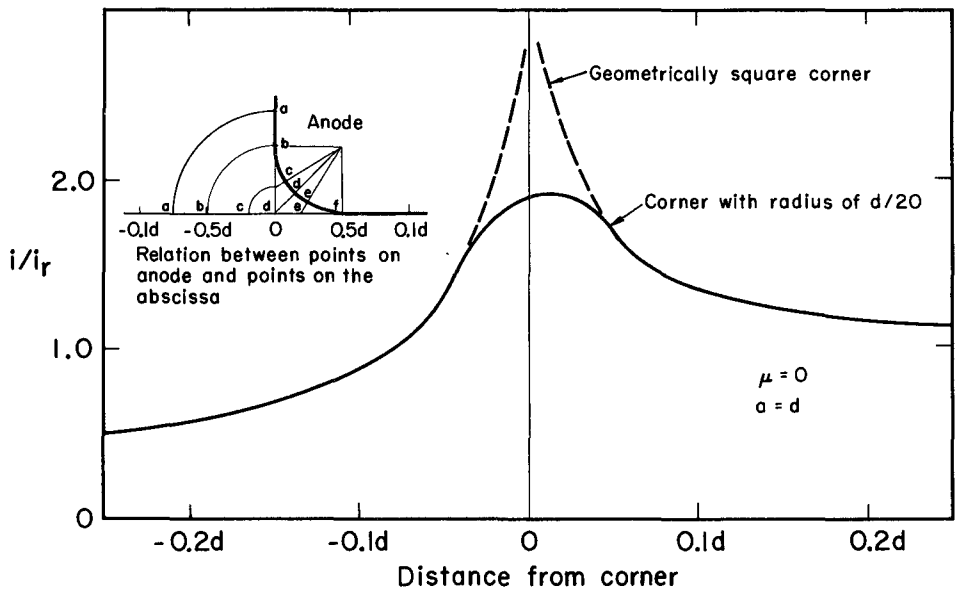

RELATIVE CURRENT DENSITY ON THE ANODE SURFACE NEAR THE CORNER

MU-31825

Fig. 8

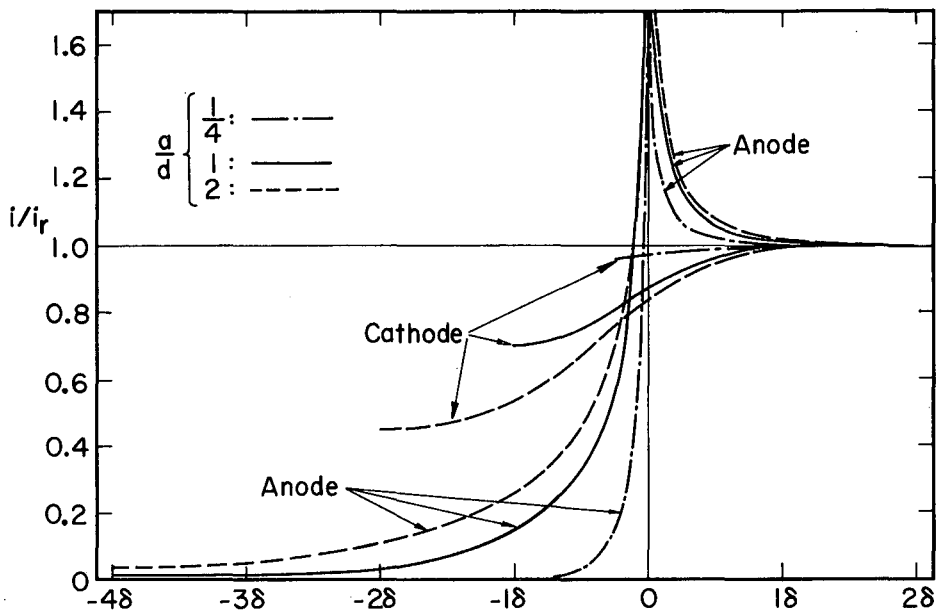
1.6
1.4
1.2
1.0
0.8
0.6
0.4
0.2
0
i/i_r
a/d
1/4
1
2
Anode
Cathode
Anode
-4δ
-3δ
-2δ
-1δ
0
1δ
2δ
EFFECT OF a/d ON DISTRIBUTION
MU-31826

Fig. 9

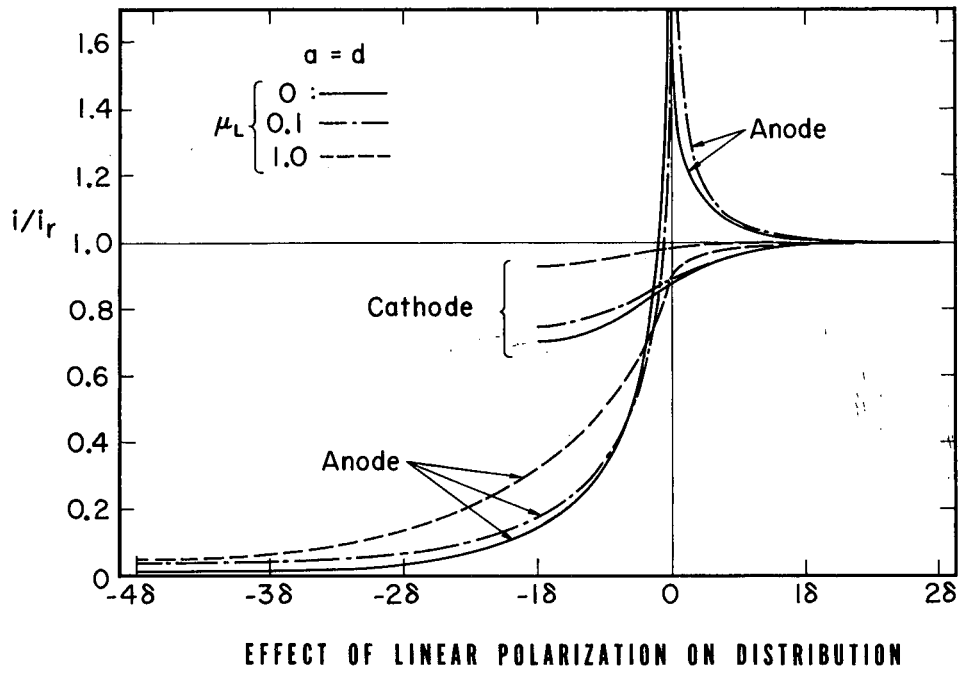

EFFECT OF LINEAR POLARIZATION ON DISTRIBUTION

MU-31827

Fig. 10

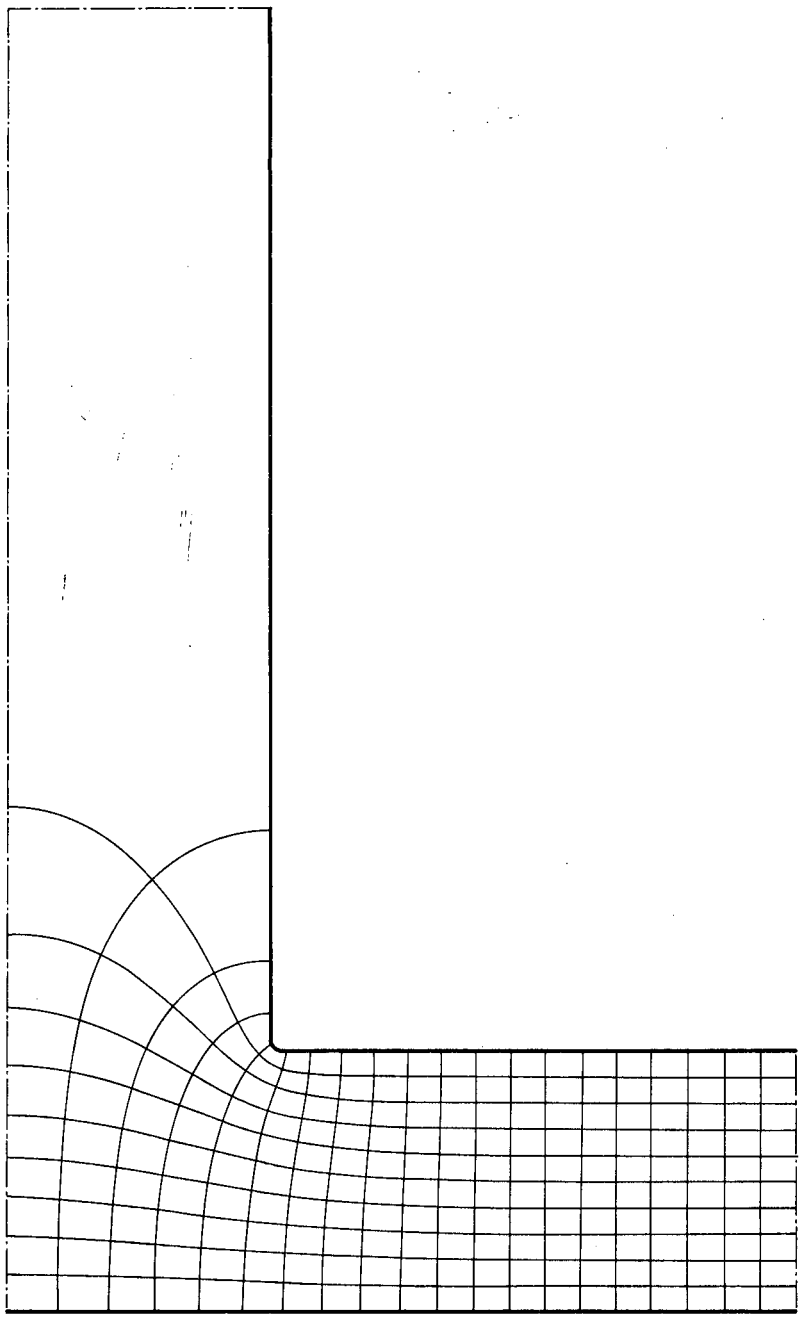

MUB-2088

Fig. 11

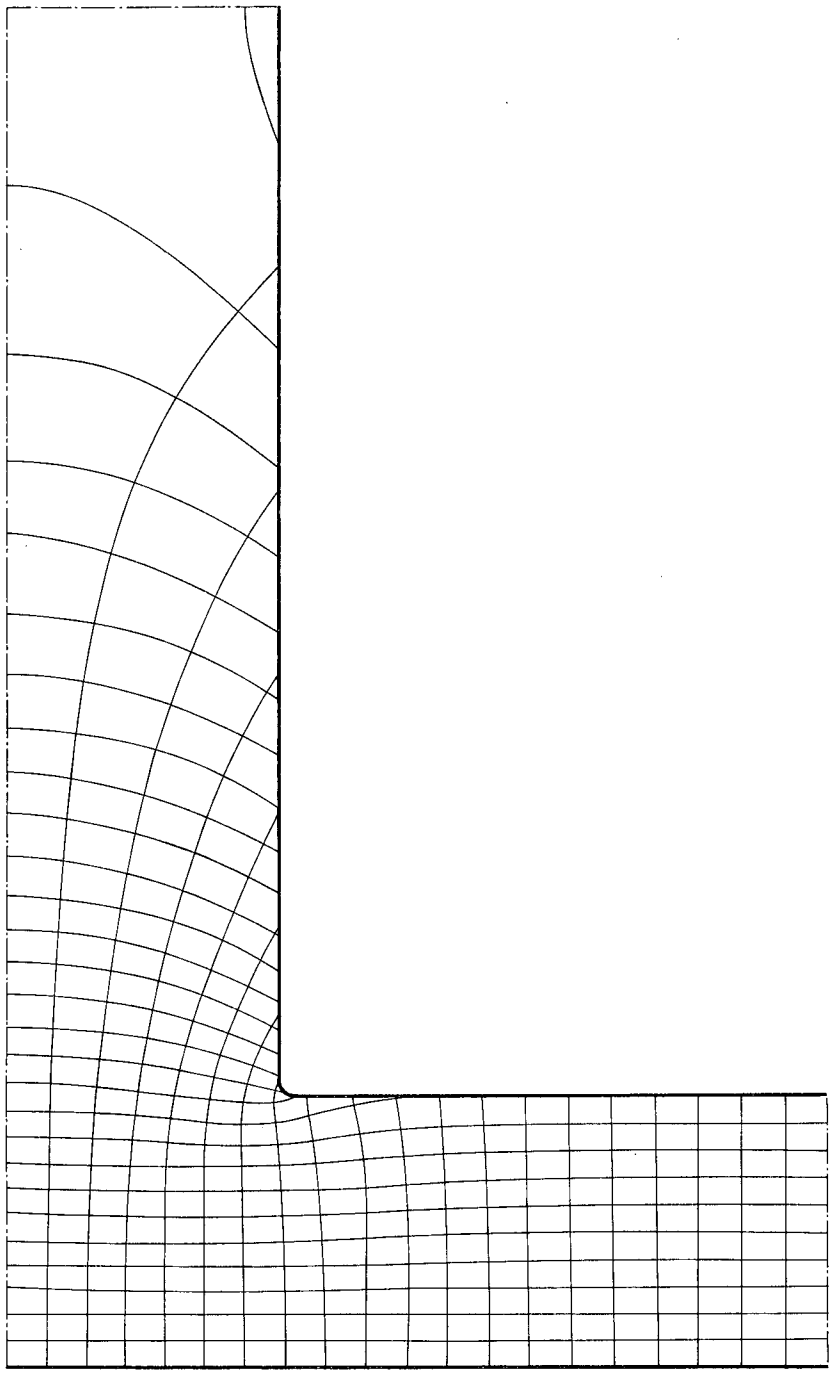

MUB-2089

Fig. 12

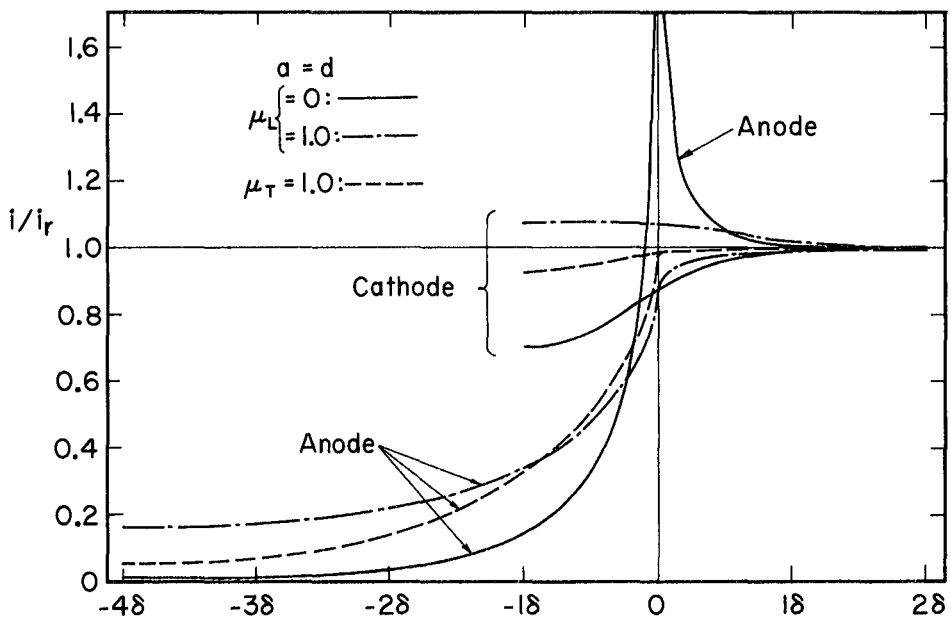

COMPARISON OF LINEAR AND TAFEL EFFECT

MU-31828

Fig. 13